Materials Physics and Mechanics 42 (2019) 1-13 Received: October 6, 2018

FINITE ELEMENT MODELLING OF CERAMOMATRIX PIEZOCOMPOSITES BY USING EFFECTIVE MODULI METHOD WITH DIFFERENT VARIANTS OF BOUNDARY CONDITIONS

G. Iovane[1], A.V. Nasedkin[2*]

[1]Department of Computer Science, University of Salerno, 84084, Fisciano (SA), Italy

[2]Institute of Mathematics, Mechanics and Computer Science, Southern Federal University, 8a, Milchakov Street, Rostov-on-Don 344090, Russia

*e-mail: nasedkin@math.sfedu.ru

Abstract. The paper presents an investigation of effective properties of piezocomposites of piezoceramic/polycrystallites type by using the effective moduli method, the computer modeling of representative volumes with random structure of granular heterogeneity and the finite element method to solve the homogenization problems. The effective moduli, obtained from the problems with different boundary conditions on the edges of representative volumes, are analyzed.

Keywords: piezoelectricity, two-phase piezocomposite, effective moduli, representative volume, finite element method, finite element software

1. Introduction

Piezoceramic composite materials have received considerable attention due to their application in sensors, actuator and other piezoelectric devices. In order to improve the efficiency of these materials, the piezoelectric composites based on piezoceramic matrices has been developed recently. Porous piezoceramic materials appeared perspective for use as the elements for acoustic transmitters and as renewable energy sources. As it turned out, in comparison with dense ceramics, porous piezoceramics had small acoustic impedance, but sufficiently high values of piezoelectric sensitivities and thickness piezomoduli. However, porous piezoceramics is less strong compared with dense ceramics. To improve the mechanical properties of porous piezoceramics, more rigid crystallites can be added into ceramic composites.

The classification of piezoelectric composites was initiated by Newnham's connectivity theory. In compliance with this theory, the ceramomatrix or polycrystalline piezocomposites can be classified as two or three phase composites with 3-0 connectivity (with closed or separate inclusions). The ceramomatrix or polycrystalline composite piezoceramic having sizes of inclusions, lesser that 100 μm may be accepted as a quasi-homogeneous medium with some effective moduli for most applications.

The material properties of porous or polymer-crystalline piezocomposites with mixed connectivities (3-0, 3-3 or 0-3) have been evaluated using different theoretical and computational models in [1–19] and others. Thus, the use of Marutake's and Bruggeman's approximations for calculation of effective moduli of piezocomposites was offered [19]. The approximate equations for elastic, dielectric and piezoelectric constants of diphasic piezocomposite form 3-0 to 3-3 connectivity were obtained in [1] based on simplified model

http://dx.doi.org/10.18720/MPM.4212019_1

combing cubes and 3-3 models. Some cubic models also were used in [2,14]. The modified cubes matrix method was proposed for analysis of the piezocomposite with different connectivity in [9] and other papers of the same authors. The dilute, self-consistent, Mori-Tanaka and differential micromechanics theories were extended in [3] to consider the effective characteristic of piezocomposite materials. The application of each theory was based on three-dimensional static solution of an ellipsoidal inclusion in an infinite piezoelectric media. Theoretical models including optimization techniques and homogenization methods have also been proposed for piezocomposite in [17].

In the present work, we have developed the effective moduli method and finite element technique in accordance with [4,5,20,21]. Theoretical aspects of the effective moduli method for inhomogeneous piezoelectric media were examined. Four static piezoelectric problems for a representative volume that allow finding the effective moduli of an inhomogeneous body were specified. These problems differ by the boundary conditions, which were set on a representative volume surfaces: mechanical displacements and electric potential ($u\varphi$), mechanical displacements and normal component of electric displacement vector (uD), mechanical stress vector and electric potential ($\sigma\varphi$), and mechanical stress vector and normal component of electric displacement vector (σD). Respective equations for calculation of effective moduli of piezoelectric media with arbitrary anisotropy were derived.

Based on these equations the full set of effective moduli for ceramomatrix composite piezoceramics having wide injection range was calculated with help of finite element method realized in the ANSYS package and in the new software ACELAN-COMPOS. Inclusions were modeled by using "granule" algorithm in ACELAN-COMPOS package. Then, the representative volume models generated in ACELAN-COMPOS were transferred to the ANSYS finite element package, where the effective moduli of the composite were calculated.

2. Mathematical models and the effective moduli method

As is known, in linear approximation for piezoelectric materials there are a linear relations between mechanical and electric fields. These dependences are called the constitutive relations and can be presented in the following four equivalent forms [22]:

$$\mathbf{T}=\mathbf{c}^{E}\cdot\mathbf{S}-\mathbf{e}^{*}\cdot\mathbf{E},\ \mathbf{D}=\mathbf{e}\cdot\mathbf{S}+\boldsymbol{\varepsilon}^{S}\cdot\mathbf{E}, \tag{1}$$

$$\mathbf{S}=\mathbf{s}^{E}\cdot\mathbf{T}+\mathbf{d}^{*}\cdot\mathbf{E},\ \mathbf{D}=\mathbf{d}\cdot\mathbf{T}+\boldsymbol{\varepsilon}^{T}\cdot\mathbf{E}, \tag{2}$$

$$\mathbf{T}=\mathbf{c}^{D}\cdot\mathbf{S}-\mathbf{h}^{*}\cdot\mathbf{D},\ \mathbf{E}=-\mathbf{h}\cdot\mathbf{S}+\boldsymbol{\beta}^{S}\cdot\mathbf{D}, \tag{3}$$

$$\mathbf{S}=\mathbf{s}^{D}\cdot\mathbf{T}+\mathbf{g}^{*}\cdot\mathbf{D},\ \mathbf{E}=-\mathbf{g}\cdot\mathbf{T}+\boldsymbol{\beta}^{T}\cdot\mathbf{D}. \tag{4}$$

Here, $\mathbf{T}=\{\sigma_{11},\sigma_{22},\sigma_{33},\sigma_{23},\sigma_{13},\sigma_{12}\}$ is the array of the mechanical stress components σ_{ij}; $\mathbf{S}=\{\varepsilon_{11},\varepsilon_{22},\varepsilon_{33},2\varepsilon_{23},2\varepsilon_{13},2\varepsilon_{12}\}$, is the array of the strain components ε_{ij}; $\mathbf{D}$ is the electric flux density vector or the vector of electric displacement; $\mathbf{E}$ is the electric field intensity vector; $\mathbf{c}^{E}$, $\mathbf{c}^{D}$ are the 6×6 matrices of elastic stiffness moduli at constant electric field and at constant electric displacement, respectively; $\mathbf{e}$, $\mathbf{d}$, $\mathbf{h}$, $\mathbf{g}$ are the 3×6 matrices of piezoelectric moduli (stress coefficients, charge coefficients, strain coefficients, voltage coefficients, respectively); $\boldsymbol{\varepsilon}^{S}$, $\boldsymbol{\varepsilon}^{T}$ are the 3×3 matrices of dielectric permittivity moduli at constant mechanical strain and at constant mechanical stress, respectively; $\mathbf{s}^{E}$, $\mathbf{s}^{D}$ are the 6×6 matrices of elastic compliance moduli at constant electric field and at constant electric displacement, respectively; $\boldsymbol{\beta}^{S}$, $\boldsymbol{\beta}^{T}$ are the 3×3 matrices of dielectric impermittivity moduli at constant mechanical strain and at constant mechanical stress, respectively; $(...)^{*}$ is the transpose operation; and $(...)\cdot(...)$ is the scalar or internal product operation. The different material constants from (1) – (4) are connected through each other by the relations:

$$\mathbf{s}^E = (\mathbf{c}^E)^{-1},\ \mathbf{s}^D = (\mathbf{c}^D)^{-1},\ \boldsymbol{\beta}^S = (\boldsymbol{\varepsilon}^S)^{-1},\ \boldsymbol{\beta}^T = (\boldsymbol{\varepsilon}^T)^{-1},\ \mathbf{c}^D = \mathbf{c}^E + \mathbf{e}^* \cdot \mathbf{h},\ \mathbf{s}^D = \mathbf{s}^E - \mathbf{d}^* \cdot \mathbf{g}, \tag{5}$$

$$\boldsymbol{\varepsilon}^T = \boldsymbol{\varepsilon}^S + \mathbf{d} \cdot \mathbf{e}^*,\ \boldsymbol{\beta}^T = \boldsymbol{\beta}^S - \mathbf{g} \cdot \mathbf{h}^*,\ \mathbf{e} = \mathbf{d} \cdot \mathbf{c}^E,\ \mathbf{d} = \boldsymbol{\varepsilon}^T \cdot \mathbf{g},\ \mathbf{g} = \boldsymbol{\beta}^T \cdot \mathbf{d},\ \mathbf{h} = \mathbf{g} \cdot \mathbf{c}^D. \tag{6}$$

Thus, if one of the sets of material moduli is known, $\{\mathbf{c}^E,\ \mathbf{e},\ \boldsymbol{\varepsilon}^S\}$, then all other sets ($\{\mathbf{s}^E,\ \mathbf{d},\ \boldsymbol{\varepsilon}^T\}$, $\{\mathbf{c}^D,\ \mathbf{h},\ \boldsymbol{\beta}^S\}$, or$\{\mathbf{s}^D,\ \mathbf{g},\ \boldsymbol{\beta}^T\}$) can be determined. In this section we show that for a composite material one can select such homogenization problems, from which we can directly determine one of the sets of effective material moduli: $\{\mathbf{c}^{E\,\mathrm{eff}},\ \mathbf{e}^{\mathrm{eff}},\ \boldsymbol{\varepsilon}^{S\,\mathrm{eff}}\}$, $\{\mathbf{s}^{E\,\mathrm{eff}},\ \mathbf{d}^{\mathrm{eff}},\ \boldsymbol{\varepsilon}^{T\,\mathrm{eff}}\}$, $\{\mathbf{c}^{D\,\mathrm{eff}},\ \mathbf{h}^{\mathrm{eff}},\ \boldsymbol{\beta}^{S\,\mathrm{eff}}\}$, $\{\mathbf{s}^{D\,\mathrm{eff}},\ \mathbf{g}^{\mathrm{eff}},\ \boldsymbol{\beta}^{T\,\mathrm{eff}}\}$.

We will consider a ceramomatrix piezocomposite as a two-phase composite in which the first phase (matrix) is a piezoceramic material, and the second phase is the elastic inclusions. Let Ω is the representative volume of heterogeneous ceramomatrix piezocomposite materials, $\Omega = \Omega^{(1)} \cup \Omega^{(2)}$; $\Omega^{(1)}$ is the volume occupied by the primary material of the matrix; $\Omega^{(2)}$ is the volume or the set of the volumes occupied by the material of the inclusions; $\Gamma = \partial\Omega$ is the boundary of the volume, $\mathbf{n}$ the vector of the external unit normal to Γ, $\mathbf{u} = \mathbf{u}(\mathbf{x})$ is the displacement vector-function, $\varphi = \varphi(\mathbf{x})$ the electric potential function, $\mathbf{x} = \{x_1,\ x_2, x_3\}$ is the vector of the Cartesian coordinates.

In order to determine the effective moduli of this composite material, we will consider four set of the homogenization problems [20, 21]. The first set is used most often and is based on the following boundary-value problem

$$\mathbf{L}^*(\nabla) \cdot \mathbf{T} = 0,\ \nabla \cdot \mathbf{D} = 0, \tag{7}$$

$$\mathbf{T} = \mathbf{c}^E \cdot \mathbf{S} - \mathbf{e}^* \cdot \mathbf{E},\ \mathbf{D} = \mathbf{e} \cdot \mathbf{S} + \boldsymbol{\varepsilon}^S \cdot \mathbf{E}, \tag{8}$$

$$\mathbf{S} = \mathbf{L}(\nabla) \cdot \mathbf{u},\ \mathbf{E} = -\nabla\varphi,\ \mathbf{L}^*(\nabla) = \begin{bmatrix} \partial_1 & 0 & 0 & 0 & \partial_3 & \partial_2 \\ 0 & \partial_2 & 0 & \partial_3 & 0 & \partial_1 \\ 0 & 0 & \partial_3 & \partial_2 & \partial_1 & 0 \end{bmatrix},\ \nabla = \begin{Bmatrix} \partial_1 \\ \partial_2 \\ \partial_3 \end{Bmatrix}, \tag{9}$$

$$\mathbf{u} = \mathbf{L}^*(\mathbf{x}) \cdot \mathbf{S}_0,\ \varphi = -\mathbf{x} \cdot \mathbf{E}_0,\ \mathbf{x} \in \Gamma, \tag{10}$$

where $\mathbf{S}_0 = \{S_{01}, S_{02}, S_{03}, S_{04}, S_{05}, S_{06}\}$; $S_{0\beta}$ are some constant values that do not depend on $\mathbf{x}$; $\mathbf{E}_0$ is some constant vector.

Note that the problem (7)–(10) should be solved in an inhomogeneous volume Ω, where $\mathbf{c}^E = \mathbf{c}^{E(j)}$, $\mathbf{e} = \mathbf{e}^{(j)}$, $\boldsymbol{\varepsilon}^S = \boldsymbol{\varepsilon}^{S(j)}$ for $\mathbf{x} \in \Omega^{(j)}$, $j = 1, 2$. We consider the elastic material of inclusions as a piezoelectric material with their elastic stiffness and dielectric permittivities moduli and with negligible piezomoduli.

In the case of ceramomatrix piezocomposite of 6*mm* class, in order to determine its ten independent effective moduli ($c_{11}^{E\,\mathrm{eff}}$, $c_{12}^{E\,\mathrm{eff}}$, $c_{13}^{E\,\mathrm{eff}}$, $c_{33}^{E\,\mathrm{eff}}$, $c_{44}^{E\,\mathrm{eff}}$, e_{31}^{eff}, e_{33}^{eff}, e_{15}^{eff}, $\varepsilon_{11}^{S\,\mathrm{eff}}$, $\varepsilon_{33}^{S\,\mathrm{eff}}$), it is enough to solve five boundary problems (7)–(10) with various values of $\mathbf{S}_0$ and $\mathbf{E}_0$, having set only one of the components $S_{0\beta}$, E_{0l} ($\beta = 1, 2, ..., 6$; $l = 1, 2, 3$) in the boundary conditions (10) not equal to zero:

$$u\varphi - \mathrm{I}.\quad S_{0\beta} = S_0\delta_{1\beta},\ \mathbf{E}_0 = 0 \Rightarrow c_{1k}^{E\,\mathrm{eff}} = \langle\sigma_{kk}\rangle / S_0;\ k = 1, 2, 3;\ e_{31}^{\mathrm{eff}} = \langle D_3\rangle / S_0, \tag{11}$$

$$u\varphi - \mathrm{II}.\quad S_{0\beta} = S_0\delta_{3\beta},\ \mathbf{E}_0 = 0 \Rightarrow c_{k3}^{E\,\mathrm{eff}} = \langle\sigma_{kk}\rangle / S_0;\ k = 1, 2, 3;\ e_{33}^{\mathrm{eff}} = \langle D_3\rangle / S_0, \tag{12}$$

$$u\varphi - \mathrm{III}.\quad S_{0\beta} = S_0\delta_{4\beta},\ \mathbf{E}_0 = 0 \Rightarrow c_{44}^{E\,\mathrm{eff}} = \langle\sigma_{23}\rangle / S_0;\ e_{15}^{\mathrm{eff}} = \langle D_2\rangle / S_0, \tag{13}$$

$$u\varphi - \mathrm{IV}.\quad \mathbf{S}_0 = 0,\ E_{0l} = E_0\delta_{1l} \Rightarrow e_{15}^{\mathrm{eff}} = -\langle\sigma_{13}\rangle / E_0;\ \varepsilon_{11}^{S\,\mathrm{eff}} = \langle D_1\rangle / E_0, \tag{14}$$

$$u\varphi - \mathrm{V}.\quad \mathbf{S}_0 = 0,\ E_{0l} = E_0\delta_{3l} \Rightarrow e_{3k}^{\mathrm{eff}} = -\langle\sigma_{kk}\rangle / E_0;\ k = 1, 2, 3;\ \varepsilon_{33}^{S\,\mathrm{eff}} = \langle D_3\rangle / E_0, \tag{15}$$

where δ_{ij} is the Kronecker symbol; and the angle brackets denote the averaged by the volume Ω values:

$$<(...)>=\frac{1}{|\Omega|}\int_{\Omega}(...)d\Omega. \tag{16}$$

The boundary conditions (8) are the linear essentially boundary conditions, which for a homogeneous piezoelectric comparison medium provide the constant stresses, electric fluxes, strains, and electric intensity fields. However, as has been shown in [20,21], we can use for the homogenization problems other boundary conditions, which also provide the constant stresses, electric fluxes, strains, and electric intensity fields for a homogeneous comparison medium.

Thus, instead of the boundary conditions (10), we can consider the natural boundary condition for the stress with known constant tensions and the essentially electric boundary condition with the known linear electric potential function:

$$\mathbf{L}^{*}(\mathbf{n})\cdot\mathbf{T}=\mathbf{L}^{*}(\mathbf{n})\cdot\mathbf{T}_0,\ \varphi=-\mathbf{x}\cdot\mathbf{E}_0,\ \mathbf{x}\in\Gamma. \tag{17}$$

Again, in the case of ceramomatrix piezocomposite of 6*mm* class, for determination full set of effective moduli ($s_{11}^{E\,\mathrm{eff}}$, $s_{12}^{E\,\mathrm{eff}}$, $s_{13}^{E\,\mathrm{eff}}$, $s_{33}^{E\,\mathrm{eff}}$, $s_{44}^{E\,\mathrm{eff}}$, d_{31}^{eff}, d_{33}^{eff}, d_{15}^{eff}, $\varepsilon_{11}^{T\,\mathrm{eff}}$, $\varepsilon_{33}^{T\,\mathrm{eff}}$), we can solve five boundary problems (5) – (7). (14) with various values of $\mathbf{T}_0$ and $\mathbf{E}_0$, having set only one of the components $T_{0\beta}$, E_{0l} ($\beta=1,2,...,6$; $l=1,2,3$) in the boundary conditions (17) not equal to zero:

$$\sigma\varphi-\mathrm{I}.\quad T_{0\beta}=T_0\delta_{1\beta},\ \mathbf{E}_0=0\ \Rightarrow\ s_{1k}^{E\,\mathrm{eff}}=\langle\varepsilon_{kk}\rangle/T_0;\ k=1,2,3;\ d_{31}^{\mathrm{eff}}=\langle D_3\rangle/T_0, \tag{18}$$

$$\sigma\varphi-\mathrm{II}.\quad T_{0\beta}=T_0\delta_{3\beta},\ \mathbf{E}_0=0\ \Rightarrow\ s_{k3}^{E\,\mathrm{eff}}=\langle\varepsilon_{kk}\rangle/T_0;\ k=1,2,3;\ d_{33}^{\mathrm{eff}}=\langle D_3\rangle/T_0, \tag{19}$$

$$\sigma\varphi-\mathrm{III}.\quad T_{0\beta}=T_0\delta_{4\beta},\ \mathbf{E}_0=0\ \Rightarrow\ s_{44}^{E\,\mathrm{eff}}=\langle\varepsilon_{23}\rangle/T_0;\ d_{15}^{\mathrm{eff}}=\langle D_2\rangle/T_0, \tag{20}$$

$$\sigma\varphi-\mathrm{IV}.\quad \mathbf{S}_0=0,\ E_{0l}=E_0\delta_{1l}\ \Rightarrow\ d_{15}^{\mathrm{eff}}=\langle\varepsilon_{13}\rangle/E_0;\ \varepsilon_{11}^{T\,\mathrm{eff}}=\langle D_1\rangle/E_0, \tag{21}$$

$$\sigma\varphi-\mathrm{V}.\quad \mathbf{S}_0=0,\ E_{0l}=E_0\delta_{3l}\ \Rightarrow\ d_{3k}^{\mathrm{eff}}=\langle\varepsilon_{kk}\rangle/E_0;\ k=1,2,3;\ \varepsilon_{33}^{T\,\mathrm{eff}}=\langle D_3\rangle/E_0. \tag{22}$$

If we assume the the essentially mechanical boundary condition with the known linear displacements and the natural electric boundary condition with known constant normal component of electric flux vector

$$\mathbf{u}=\mathbf{L}^{*}(\mathbf{x})\cdot\mathbf{S}_0,\ \mathbf{n}\cdot\mathbf{D}=\mathbf{n}\cdot\mathbf{D}_0,\ \mathbf{x}\in\Gamma, \tag{23}$$

then for transversely isotropic ceramomatrix piezocomposite we can solve five boundary problems (7) – (9), (23) with various values of $\mathbf{S}_0$ and $\mathbf{D}_0$, having set only one of the components $S_{0\beta}$, D_{0l} ($\beta=1,2,...,6$; $l=1,2,3$) in (23) not equal to zero, and from the solution of these problems we directly obtain the effective moduli $c_{11}^{D\,\mathrm{eff}}$, $c_{12}^{D\,\mathrm{eff}}$, $c_{13}^{D\,\mathrm{eff}}$, $c_{33}^{D\,\mathrm{eff}}$, $c_{44}^{D\,\mathrm{eff}}$, h_{31}^{eff}, h_{33}^{eff}, h_{15}^{eff}, $\beta_{11}^{S\,\mathrm{eff}}$, $\beta_{33}^{S\,\mathrm{eff}}$:

$$uD-\mathrm{I}.\quad S_{0\beta}=S_0\delta_{1\beta},\ \mathbf{D}_0=0\ \Rightarrow\ c_{1k}^{D\,\mathrm{eff}}=\langle\sigma_{kk}\rangle/S_0;\ k=1,2,3;\ h_{31}^{\mathrm{eff}}=-\langle E_3\rangle/S_0, \tag{24}$$

$$uD-\mathrm{II}.\quad S_{0\beta}=S_0\delta_{3\beta},\ \mathbf{D}_0=0\ \Rightarrow\ c_{k3}^{D\,\mathrm{eff}}=\langle\sigma_{kk}\rangle/S_0;\ k=1,2,3;\ h_{33}^{\mathrm{eff}}=-\langle E_3\rangle/S_0, \tag{25}$$

$$uD-\mathrm{III}.\quad S_{0\beta}=S_0\delta_{4\beta},\ \mathbf{D}_0=0\ \Rightarrow\ c_{44}^{D\,\mathrm{eff}}=\langle\sigma_{23}\rangle/S_0;\ h_{15}^{\mathrm{eff}}=-\langle E_2\rangle/S_0, \tag{26}$$

$$uD-\mathrm{IV}.\quad \mathbf{S}_0=0,\ D_{0l}=D_0\delta_{1l}\ \Rightarrow\ h_{15}^{\mathrm{eff}}=-\langle\sigma_{13}\rangle/D_0;\ \beta_{11}^{S\,\mathrm{eff}}=\langle E_1\rangle/D_0, \tag{27}$$

$$uD-\mathrm{V}.\quad \mathbf{S}_0=0,\ D_{0l}=D_0\delta_{3l}\ \Rightarrow\ h_{3k}^{\mathrm{eff}}=-\langle\sigma_{kk}\rangle/D_0;\ k=1,2,3;\ \beta_{33}^{S\,\mathrm{eff}}=\langle E_3\rangle/D_0. \tag{28}$$

At last, we can consider the natural mechanical and electric boundary conditions with the known constant tensions and the normal component of electric flux vector:

$$\mathbf{L}^{*}(\mathbf{n})\cdot\mathbf{T}=\mathbf{L}^{*}(\mathbf{n})\cdot\mathbf{T}_0,\ \mathbf{n}\cdot\mathbf{D}=\mathbf{n}\cdot\mathbf{D}_0,\ \mathbf{x}\in\Gamma. \tag{29}$$

Now for transversely isotropic ceramomatrix piezocomposite we solve five boundary problems (7) – (9), (29) with various values of $\mathbf{T}_0$ and $\mathbf{D}_0$, having set in (29) only one nonzero components $T_{0\beta}$, D_{0l} ($\beta = 1, 2, ..., 6$; $l = 1, 2, 3$), and after solving these problems we at first obtain the effective moduli $s_{11}^{D\,\mathrm{eff}}$, $s_{12}^{D\,\mathrm{eff}}$, $s_{13}^{D\,\mathrm{eff}}$, $s_{33}^{D\,\mathrm{eff}}$, $s_{44}^{D\,\mathrm{eff}}$, g_{31}^{eff}, g_{33}^{eff}, g_{15}^{eff}, $\beta_{11}^{T\,\mathrm{eff}}$, $\beta_{33}^{T\,\mathrm{eff}}$:

$$\sigma D - \mathrm{I}.\quad T_{0\beta} = T_0\delta_{1\beta},\ \mathbf{D}_0 = 0 \Rightarrow s_{1k}^{D\,\mathrm{eff}} = \langle \varepsilon_{kk} \rangle / T_0;\ k = 1, 2, 3;\ g_{31}^{\mathrm{eff}} = -\langle E_3 \rangle / T_0, \tag{30}$$

$$\sigma D - \mathrm{II}.\quad T_{0\beta} = T_0\delta_{3\beta},\ \mathbf{D}_0 = 0 \Rightarrow s_{k3}^{D\,\mathrm{eff}} = \langle \varepsilon_{kk} \rangle / T_0;\ k = 1, 2, 3;\ g_{33}^{\mathrm{eff}} = -\langle E_3 \rangle / T_0, \tag{31}$$

$$\sigma D - \mathrm{III}.\quad T_{0\beta} = T_0\delta_{4\beta},\ \mathbf{D}_0 = 0 \Rightarrow s_{44}^{D\,\mathrm{eff}} = \langle \varepsilon_{23} \rangle / T_0;\ g_{15}^{\mathrm{eff}} = -\langle E_2 \rangle / T_0, \tag{32}$$

$$\sigma D\, q - \mathrm{IV}.\quad \mathbf{T}_0 = 0,\ D_{0l} = D_0\delta_{1l} \Rightarrow g_{15}^{\mathrm{eff}} = \langle \varepsilon_{13} \rangle / D_0;\ \beta_{11}^{T\,\mathrm{eff}} = \langle E_1 \rangle / D_0, \tag{33}$$

$$\sigma D - \mathrm{V}.\quad \mathbf{T}_0 = 0,\ D_{0l} = D_0\delta_{3l} \Rightarrow g_{3k}^{\mathrm{eff}} = \langle \varepsilon_{kk} \rangle / D_0;\ k = 1, 2, 3;\ \beta_{33}^{T\,\mathrm{eff}} = \langle E_3 \rangle / D_0. \tag{34}$$

For each set of these problems from found effective moduli we can calculate for "equivalent" effective homogeneous medium the other moduli from the constitutive equations (1) – (4) and the relations (5), (6). We note, that effective moduli, found from different problems $u\varphi$, $\sigma\varphi$, uD, and σD, will differ, i.e. $(\mathbf{c}^{E\,\mathrm{eff}})_{u\varphi} \neq (\mathbf{c}^{E\,\mathrm{eff}})_{\sigma\varphi} \neq (\mathbf{c}^{E\,\mathrm{eff}})_{uD} \neq (\mathbf{c}^{E\,\mathrm{eff}})_{\sigma D}$, etc.

Further, all these problems will be solved in a representative volume Ω numerically by the finite element method.

3. Averaging of inclusions for polycrystalline piezoceramic

For the case of polycrystalline elastic inclusions, we must calculate at the first stage the effective moduli for material of inclusions. At the next stage, we will study piezocomposite with isotropic inclusions as two-phase composite according to the approaches described above. As an example, we shall consider PZT/α–Al_2O_3 composite material.

For calculation of average moduli of inclusions, we shall take into account, that inclusions represent the crystallites of sapphire (α-corundum) Al_2O_3. These inclusions are the crystals of system $\bar{3}m$ [23], which crystallographic axes are oriented in random manner with respect to the global Cartesian coordinate system. In crystallographic axes, its moduli have the following structure

$$\mathbf{c}^r = \begin{bmatrix} c_{11}^r & c_{12}^r & c_{13}^r & c_{14}^r & 0 & 0 \\ c_{12}^r & c_{11}^r & c_{13}^r & -c_{14}^r & 0 & 0 \\ c_{13}^r & c_{13}^r & c_{33}^r & 0 & 0 & 0 \\ c_{14}^r & -c_{14}^r & 0 & c_{44}^r & 0 & 0 \\ 0 & 0 & 0 & 0 & c_{44}^r & c_{14}^r \\ 0 & 0 & 0 & 0 & c_{14}^r & c_{66}^r \end{bmatrix}, \qquad \boldsymbol{\varepsilon}^r = \begin{bmatrix} \varepsilon_{11}^r & 0 & 0 \\ 0 & \varepsilon_{11}^r & 0 \\ 0 & 0 & \varepsilon_{33}^r \end{bmatrix},$$

where $c_{66}^r = (c_{11}^r - c_{12}^r)/2$.

In this connection, the effective moduli can be defined as the average moduli of monophase polycrystallite of trigonal system [21]. Here, the averaging of crystallites moduli on every of the possible orientations of crystallographic axes can be implemented in implicit form [24]. As a result, the inclusions can be considered as isotropic material, which effective moduli are expressed through the initial stiffness moduli $c_{\alpha\beta}^r$ and the flexibility or compliance moduli $s_{\alpha\beta}^r$ under well-known formulas [24].

The Voight's averaging gives the following values for the effective bulk module $K_V^{(2)}$ and shear module $\mu_V^{(2)}$

$$K_V^{(2)} = \frac{1}{9}\sum_{\alpha=1}^{3}\sum_{\beta=1}^{3} c_{\alpha\beta}^r, \qquad \mu_V^{(2)} = \frac{1}{30}\left(3\sum_{\alpha=1}^{3} c_{\alpha\alpha}^r + 6\sum_{\alpha=4}^{6} c_{\alpha\alpha}^r - \sum_{\alpha=1}^{3}\sum_{\beta=1}^{3} c_{\alpha\beta}^r\right),$$

Alternative averaging on Reuss for flexibility or compliance tensors allows one to find the inverse values for the effective moduli $K_R^{(2)}$ and $\mu_R^{(2)}$:

$$(K_R^{(2)})^{-1} = \sum_{\alpha=1}^{3}\sum_{\beta=1}^{3} s_{\alpha\beta}^r, \quad (\mu_R^{\text{eff}})^{-1} = \frac{1}{15}\left(6\sum_{\alpha=1}^{3} s_{\alpha\alpha}^r + 3\sum_{\alpha=4}^{6} s_{\alpha\alpha}^r - 2\sum_{\alpha=1}^{3}\sum_{\beta=1}^{3} s_{\alpha\beta}^r\right),$$

At the averaging of trigonal system polycrystallite the given formulas can be rewritten in the form [24]:

$$K_V^{(2)} = \frac{1}{9}(2c_{11}^r + c_{33}^r + 2(c_{12}^r + 2c_{13}^r)),\ \mu_V^{(2)} = \frac{1}{30}(7c_{11}^r + 2c_{33}^r - 5c_{12}^r - 4c_{13}^r + 12c_{44}^r), \tag{35}$$

$$(K_R^{(2)})^{-1} = 2s_{11}^r + s_{33}^r + 2(s_{12}^r + 2s_{13}^r),\ (\mu_R^{(2)})^{-1} = \frac{2}{15}(7s_{11}^r + 2s_{33}^r - 5s_{12\alpha}^r - 4s_{13}^r + 3s_{44}^r). \tag{36}$$

According to the Hill's approach for the final values of effective moduli of a monophase polycrystalline material, we shall take the arithmetic middling values obtained by averaging on Voight and Reuss:

$$K^{(2)} = (K_V^{(2)} + K_R^{(2)})/2,\ \mu^{(2)} = (\mu_V^{(2)} + \mu_R^{(2)})/2. \tag{37}$$

Then, the average values of Young's module $E^{(2)}$, Poisson's coefficient $\nu^{(2)}$, and stiffness moduli $c_{11}^{(2)}$, $c_{12}^{(2)}$ for inclusion material can be found by using the standard formulas from $K^{(2)}$ and $\mu^{(2)}$

$$E^{(2)} = \frac{9K^{(2)}\mu^{(2)}}{(3K^{(2)} + \mu^{(2)})},\ \nu^{(2)} = \frac{(3K^{(2)} - \mu^{(2)})}{(6K^{(2)} + 2\mu^{(2)})}. \tag{38}$$

$$c_{11}^{(2)} = \frac{(1-\nu^{(2)})E^{(2)}}{(1+\nu^{(2)})(1-2\nu^{(2)})},\ c_{12}^{(2)} = \frac{\nu^{(2)}E^{(2)}}{(1+\nu^{(2)})(1-2\nu^{(2)})}. \tag{39}$$

The averaging of dielectric permittivities on every of the possible orientations of crystallographic axes leads to isotropic dielectric medium with effective permittivity $\varepsilon^{(2)}$:

$$\varepsilon^{\text{eff}} = (2\varepsilon_{11}^r + \varepsilon_{33}^r)/2. \tag{40}$$

Thus, the inclusions from sapphire crystallites of trigonal system can be modelled by isotropic material with effective elastic moduli $E^{(2)}$, $\nu^{(2)}$ or $c_{11}^{(2)}$, $c_{12}^{(2)}$ and dielectric permittivitie $\varepsilon^{(2)}$, expressed by moduli of sapphire $c_{\alpha\beta}^r$, $s_{\alpha\beta}^r$, ε_{ii}^r from formulas (35) – (40).

4. Models of representative volumes

As a representative volume element, we consider a cube evenly divided into smaller piezoelectric cubic finite elements with eight nodes. For a mixed two-phase composite, such element can have piezoelectric properties of the first phase or of the second phase. We use the 3-0 algorithm from ACELAN-COMPOS package for simulation of inclusions as granules, consisting of one or more structural elements not connected with other granules [25–27]. In this algorithm, the representative volumes consist of domains with $8\times8\times8$ elements. Number 8 for the domain division was chosen for the convenience of implementing numerical procedures to generate data structures and verify the phase connectivity.

The input user data are the boundary granule size and the maximum quantum of inclusions in the representative volume. Random choice of the supporting element for the granules ensures in the result the stochastic distribution of material properties in the representative volume element. The granule grows in the domain of $8\times8\times8$ element size according to an algorithm that allows the granule to be shaped as close to the ball as possible, while avoiding highly elongated elements.

Each domain is created by a partially random way, and the representative volumes of $8m\times8m\times8m$ order are formed in the result of generating the sequence of domains along three coordinate axes. Thus, each resulting domain differs from the other. Nevertheless, it maintains the connectivity of the main phase and the connectivity of the total volume structure, formed by a 3-0 connectivity algorithm from ACELAN-COMPOS package. A detailed description of this algorithm is contained in [26,27].

Some examples of the representative volume element for $m=2$ (eight domains) and for $m=3$ (twenty seven domains) are shown in Fig. 1 and Fig. 2, respectively. In these figures the cases (*a*) and (*b*) correspond to the percentage of inclusions $p=10$ %, and the cases (*c*) and (*d*) correspond to the percentage of inclusions $p=60$ %.

At the next step, the generated structures were transferred to ANSYS finite element package, where all further operations were carried out.

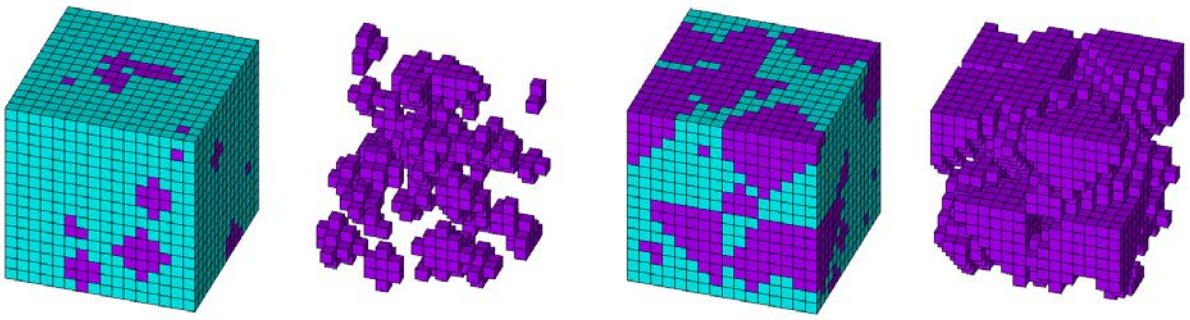

(*a*) (*b*) (*c*) (*d*)

Fig. 1. Example of a representative volume elements $16\times16\times16$: (*a*) whole volume with 10 % of inclusions, (*b*) elastic elements in volume with 10 % of inclusions, (*c*) whole volume with 60 % of inclusions, (*d*) elastic elements in volume with 60 % of inclusions

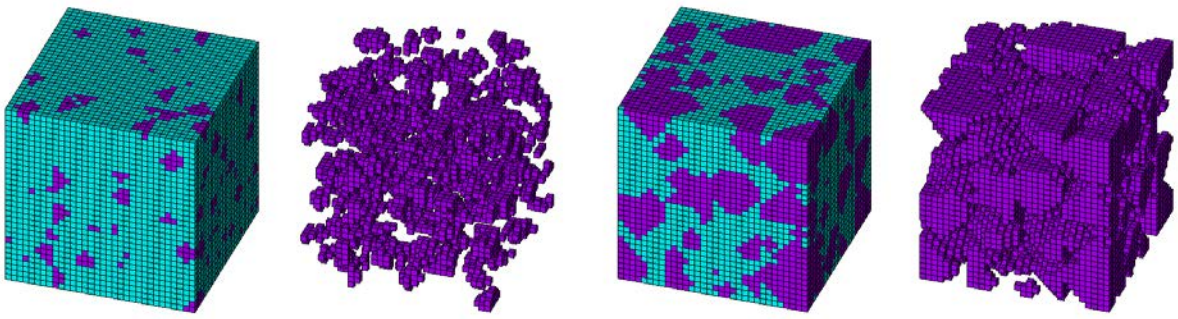

(*a*) (*b*) (*c*) (*d*)

Fig. 2. Example of a representative volume elements $32\times32\times32$: (*a*) whole volume with 10 % of inclusions, (*b*) elastic elements in volume with 10 % of inclusions, (*c*) whole volume with 60 % of inclusions, (*d*) elastic elements in volume with 60 % of inclusions

Then, the problems (7) – (9) with (10), (17), (23) or (29) were solved for the representative volume using finite element technology and ANSYS package. In the end, in the ANSYS postprocessor the average characteristics (stresses, strains, electric fluxes and electric intensity fields) were automatically calculated by (16) according to (11) – (15), (18) – (22), (24) – (28), or (30) – (34), and thus the full sets of the effective material moduli of piezocomposite were obtained. We used an eight-node finite element SOLID5 with the displacements and the electric potential as degrees of freedom in each node and with capability of piezoelectric analysis. Computing experiments were performed in ANSYS software of 11.0 version. However, the developed programs in macrolanguage APDL ANSYS will work in higher versions of ANSYS that support piezoelectric analysis and finite element SOLID5.

5. Numerical examples

To provide an example, we consider a PCR-1/α–Al_2O_3 composite material. For the dense piezoceramic PCR-1 we take the following values of material constants [28]: $c_{11}^{E(1)} = 15.3 \cdot 10^{10}$, $c_{12}^{E(1)} = 8.7 \cdot 10^{10}$, $c_{13}^{E(1)} = 8.7 \cdot 10^{10}$, $c_{33}^{E(1)} = 12.7 \cdot 10^{10}$, $c_{44}^{E(1)} = 2.6 \cdot 10^{10}$ $\left(N/m^2\right)$, $e_{31}^{(1)} = -2.1$, $e_{33}^{(1)} = 12.4$, $e_{15}^{(1)} = 11.3$ (C/m^2); $\varepsilon_{11}^{S(1)} = 572\varepsilon_0$, $\varepsilon_{33}^{S(1)} = 304\varepsilon_0$, where $\varepsilon_0 = 8.85 \cdot 10^{-12}$ (F/m) is the dielectric permittivity of the vacuum. We assume the following values of material moduli of sapphire [29]: $c_{11}^{r} = 49.7 \cdot 10^{10}$, $c_{12}^{r} = 16.3 \cdot 10^{10}$, $c_{13}^{r} = 11.1 \cdot 10^{10}$, $c_{33}^{r} = 49.8 \cdot 10^{10}$, $c_{44}^{r} = 14.7 \cdot 10^{10}$, $c_{14}^{r} = -2.35 \cdot 10^{10}$ $\left(N/m^2\right)$, $\varepsilon_{11}^{r} = 9.34\varepsilon_0$, $\varepsilon_{33}^{r} = 11.54\varepsilon_0$. Then, after the calculation by formulas (32)–(37) we obtain the averaging moduli of (α-corundum as an isotropic phase: $E^{(2)} = 40.26 \cdot 10^{10}$ (N/m^2); $\nu^{(2)} = 0.23$; $c_{11}^{(2)} = 46.88 \cdot 10^{10}$ (N/m^2), $c_{12}^{(2)} = 14.22 \cdot 10^{10}$ (N/m^2); $\varepsilon^{(2)} = \varepsilon^{\text{eff}} = 10\varepsilon_0$. For the representative volume, we take $8m \times 8m \times 8m$ element structures with number $m = 3$, which provide close convergence of the computational results.

We are going to analyze the relative effective moduli. For example, $r(c_{\alpha\beta}^{E\,\text{eff}}) = c_{\alpha\beta}^{E\,\text{eff}} / c_{\alpha\beta}^{E}$ are the values of the effective moduli $c_{\alpha\beta}^{E\,\text{eff}}$, related to the corresponding values of the moduli $c_{\alpha\beta}^{E}$ for the dense piezoceramic without inclusions, and so on.

Table 1 shows the effective elastic stiffness moduli with a different percentage of inclusions for $u\varphi$-problems (7) – (15), $\sigma\varphi$-problems (7) – (9), (17) – (22), uD-problems (7)–(9), (23) – (28), and σD-problems (7) – (9), (29) – (34).

Table 1. Relative values of effective elastic stiffness moduli

Relative moduli	Boundary problem	Percentage of inclusions					
		10	20	30	40	50	60
$r(c_{11}^{E\,\text{eff}})$	$u\varphi$	1.128	1.261	1.406	1.581	1.767	1.931
	$\sigma\varphi$	1.116	1.222	1.352	1.502	1.676	1.837
	uD	1.128	1.261	1.407	1.581	1.767	1.933
	σD	1.115	1.225	1.352	1.505	1.683	1.842
$r(c_{12}^{E\,\text{eff}})$	$u\varphi$	1.047	1.098	1.146	1.198	1.254	1.310
	$\sigma\varphi$	1.051	1.102	1.157	1.208	1.275	1.314
	uD	1.047	1.098	1.146	1.198	1.254	1.311
	σD	1.049	1.108	1.153	1.210	1.284	1.316
$r(c_{13}^{E\,\text{eff}})$	$u\varphi$	1.048	1.099	1.147	1.191	1.250	1.295

	$\sigma\varphi$	1.054	1.101	1.168	1.208	1.254	1.318
	uD	1.049	1.100	1.147	1.190	1.247	1.289
	σD	1.051	1.098	1.157	1,197	1.245	1.297
$r(c_{33}^{E\,\mathrm{eff}})$	$u\varphi$	1.193	1.391	1.618	1.843	2.083	2.337
	$\sigma\varphi$	1.170	1.315	1.529	1.713	1.932	2.179
	uD	1.195	1.397	1.629	1.860	2.101	2.367
	σD	1.176	1.335	1.556	1.759	1.984	2.259
$r(c_{44}^{E\,\mathrm{eff}})$	$u\varphi$	1.336	1.708	2.134	2.542	3.055	3.550
	$\sigma\varphi$	1.278	1.564	1.896	2.250	2.697	3.157
	uD	1.341	1.725	2.159	2.580	3.106	3.608
	σD	1.294	1.595	1.972	2.341	2.815	3.328

Tables 2, 3 and 4 present similar results for effective piezoelectric moduli (stress coefficients) e_{31}^{eff}, e_{33}^{eff}, and e_{15}^{eff}, effective dielectric permittivity moduli $\varepsilon_{11}^{S\,\mathrm{eff}}$, $\varepsilon_{33}^{S\,\mathrm{eff}}$, and effective piezoelectric moduli (charge coefficients) d_{31}^{eff}, d_{33}^{eff}, and d_{15}^{eff}, respectively. Note that the values of piezoelectric charge coefficients have a significant influence on the performance of piezoelectric devices, especially for hydroacoustic applications.

Table 2. Relative values of effective piezoelectric moduli (stress coefficients)

Relative moduli	Boundary problem	Percentage of inclusions					
		10	20	30	40	50	60
$r(e_{31}^{\mathrm{eff}})$	$u\varphi$	0.956	0.907	0.830	0.727	0.620	0.509
	$\sigma\varphi$	0.977	0.936	0.909	0.814	0.693	0.624
	uD	0.959	0.914	0.834	0.727	0.610	0.470
	σD	0.968	0.909	0.863	0.758	0.626	0.520
$r(e_{33}^{\mathrm{eff}})$	$u\varphi$	0.897	0.788	0.676	0.574	0.473	0.376
	$\sigma\varphi$	0.909	0.828	0.723	0.641	0.545	0.448
	uD	0.892	0.778	0.659	0.547	0.444	0.324
	σD	0.900	0.806	0.689	0.588	0.487	0.351
$r(e_{15}^{\mathrm{eff}})$	$u\varphi$	0.898	0.787	0.660	0.572	0.468	0.347
	$\sigma\varphi$	0.912	0.822	0.719	0.639	0.527	0.433
	uD	0.893	0.772	0.638	0.541	0.425	0.298
	σD	0.903	0.798	0.675	0.584	0.459	0.339

Table 3. Relative values of effective dielectric permittivity moduli

Relative moduli	Boundary problem	Percentage of inclusions					
		10	20	30	40	50	60
$r(\varepsilon_{11}^{S\,\mathrm{eff}})$	$u\varphi$	0.872	0.741	0.608	0.511	0.415	0.308
	$\sigma\varphi$	0.875	0.755	0.619	0.528	0.435	0.325
	uD	0.867	0.727	0.589	0.484	0.378	0.268
	σD	0.870	0.736	0.600	0.497	0.389	0.279
$r(\varepsilon_{33}^{S\,\mathrm{eff}})$	$u\varphi$	0.883	0.765	0.652	0.551	0.454	0.364
	$\sigma\varphi$	0.887	0.775	0.665	0.569	0.472	0.382
	uD	0.880	0.758	0.640	0.532	0.434	0.323
	σD	0.882	0.765	0.647	0.543	0.443	0.329

Table 4. Relative values of effective piezoelectric moduli (charge coefficients)

Relative moduli	Boundary problem	Percentage of inclusions					
		10	20	30	40	50	60
$r(d_{31}^{\text{eff}})$	$u\varphi$	0.645	0.444	0.304	0.210	0.146	0.100
	$\sigma\varphi$	0.690	0.517	0.374	0.271	0.188	0.137
	uD	0.641	0.438	0.297	0.201	0.139	0.087
	σD	0.675	0.488	0.344	0.239	0.161	0.104
$r(d_{33}^{\text{eff}})$	$u\varphi$	0.650	0.448	0.306	0.214	0.150	0.103
	$\sigma\varphi$	0.692	0.521	0.370	0.273	0.194	0.138
	uD	0.645	0.440	0.297	0.203	0.140	0.087
	σD	0.676	0.492	0.340	0.240	0.166	0.103
$r(d_{15}^{\text{eff}})$	$u\varphi$	0.672	0.461	0.309	0.225	0.153	0.098
	$\sigma\varphi$	0.714	0.526	0.379	0.284	0.195	0.137
	uD	0.666	0.447	0.295	0.210	0.137	0.083
	σD	0.697	0.500	0.342	0.249	0.163	0.102

For piezocomposite with soft inclusions, we have obtained the following results. The models ($u\varphi$) and (uD), in which fixation conditions are pointed out, are more rigid than the models ($\sigma\varphi$) and (σD), in which mechanical stresses are fixed. Therefore, the effective stiffness moduli for models with specified displacements are greater than for models with specified stresses, i.e. $(c_{\alpha\beta}^{E\,\text{eff}})_{\sigma\xi} < (c_{\alpha\beta}^{E\,\text{eff}})_{u\xi}$, $\xi = \varphi, D$. At the same time, the influence of electric boundary conditions on the stiffness moduli is extremely insignificant.

For effective dielectric permittivity moduli the following inequalities hold: $(\varepsilon_{ii}^{S\,\text{eff}})_{uD} < (\varepsilon_{ii}^{S\,\text{eff}})_{\sigma D} < (\varepsilon_{ii}^{S\,\text{eff}})_{u\varphi} < (\varepsilon_{ii}^{S\,\text{eff}})_{\sigma\varphi}$. Thus, the dielectric constants are the highest for the model with specified stresses and electric potential. Note that the differences in the values of the effective dielectric permittivity moduli increase as the percentage of the non-piezoelectric phase increases.

The inequalities for effective piezoelectric stress coefficients somewhat differ from their inequalities for effective dielectric permittivity moduli: $(e_{33}^{\text{eff}})_{uD} < (e_{33}^{\text{eff}})_{u\varphi} < (e_{33}^{\text{eff}})_{\sigma D} < (e_{33}^{\text{eff}})_{\sigma\varphi}$, $(e_{15}^{\text{eff}})_{uD} < (e_{15}^{\text{eff}})_{u\varphi} < (e_{15}^{\text{eff}})_{\sigma D} < (e_{15}^{\text{eff}})_{\sigma\varphi}$, $(|e_{31}^{\text{eff}}|)_{u\varphi} < (|e_{31}^{\text{eff}}|)_{uD} < (|e_{31}^{\text{eff}}|)_{\sigma D} < (|e_{31}^{\text{eff}}|)_{\sigma\varphi}$. It can be seen that both the values of the piezomoduli and the values of the dielectric constants are maximum for the $\sigma\varphi$-problem. The differences in the values of the effective piezoelectric stress coefficients also increase as the fraction of the elastic inclusions increases.

The inequalities for nonzero effective piezoelectric charge coefficients almost repeat the corresponding inequalities for effective piezoelectric stress coefficients: $(|d_{i\alpha}^{\text{eff}}|)_{uD} < (|d_{i\alpha}^{\text{eff}}|)_{u\varphi} < (|d_{i\alpha}^{\text{eff}}|)_{\sigma D} < (|d_{i\alpha}^{\text{eff}}|)_{\sigma\varphi}$. Note that the choice of boundary conditions has the greatest influence on the piezoelectric charge coefficients, and the relative differences between the values of these piezomoduli can reach 50 %.

6. Conclusions

Thus, in present paper we develop the effective moduli method and finite element technique in accordance with [20, 21]. To find the effective moduli of an inhomogeneous body, we set four static piezoelectric problems for a representative volume. These problems differ by the boundary conditions, which are set on the representative volume surfaces, and which guarantee the constant values of electric displacements, strains, stresses and electric fields for homogeneous material. Special formulas are derived to calculate the effective moduli of piezoelectric media with arbitrary anisotropy. Based on these formulas, we find the full set of

effective moduli for ceramic polycrystalline piezocomposites using finite element method. The finite element computations were implemented using the computation package ANSYS, and specially developed computer programs were written in macrolanguage APDL ANSYS. At that, the generation of the granular structures for representative volumes was carried out using separate finite element software ACELAN-COMPOS.

As a representative volume, we consider a cube evenly divided into cubic piezoelectric finite elements. At the first stage, depending on the given percentage of inclusions the material properties, selected by special granular algorithm ACELAN-COMPOS finite elements, are modified to the properties of inclusions. Further from the solutions of homogenization problems, we determine the effective moduli of the piezocomposite made of piezoceramics and crystallites. To provide an example, we consider polycrystalline piezoceramics with sapphire (α-corundum) crystallites Al_2O_3 as inclusions. The effective moduli for inclusions are calculated as the average moduli of monophase polycrystallite of trigonal system. The results of calculations give the full set of effective moduli.

We note that the results obtained here differ from the results presented in [16,30,31]. In particular, we did not obtain a growth of the piezoelectric modulus d_{33}^{eff} in the range of 0–20 % of the inclusions. These differences are due to that the porous ceramomatrix composites were studied in [16,30,31]. Thus, the optical photomicrographs of the polished surface of these piezocomposites, obtained in the Research Institute of Physics from Southern Federal University [16,30], are shown in Fig. 3.

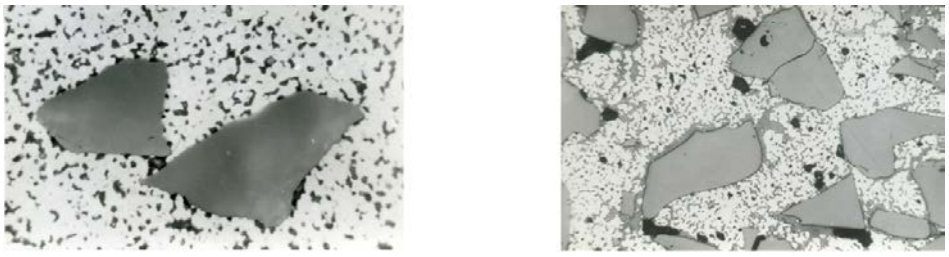

Fig. 3. Optical photomicrographs of porous ceramomatrix piezocomposites with different percentage of inclusion

From these figures, it can be seen that the pores in piezoceramics are ten times smaller than the sizes of crystallites. Therefore, for such complex three-phase material the homogenization can be carried out in two stages. At the first stage, the effective moduli of porous piezoceramics can be calculated, and at the second stage, the effective moduli of two-phase composite ceramic/crystallites can be determined. Then, for modelling the porous piezoceramics, one can use the models developed in [32–35], where pores were considered as voids, as well as the models of inhomogeneous polarization near the pore boundary [20]. We plan that these approaches will be the subject of further research.

Acknowledgements. *This research for second author was supported by the Ministry of Education and Science of Russia, competitive part of the state assignment, No. 9.1001.2017/4.6, and the project "Organization of scientific research", No. 9.5070.2017/6.7.*

References

[1] Banno H. Effect of shape and volume fraction of closed pores on dielectric, elastic and electromechanical properties of dielectric and piezoelectric ceramics - a theoretical approach. *Amer. Ceram. Soc. Bull*. 1987;66(9): 1332-1337.

[2] Bowen CR, Perry A, Kara H, Mahon SW. Analytical modelling of 3-3 piezoelecrtic composites. *J. Eur. Ceram. Soc*. 2001;21(10-11): 1463-1467.

[3] Dunn H, Taya M. Electromechanical properties of porous piezoelectric ceramics. *J. Am. Ceram. Soc*. 1993;76(7): 1697-1706.
[4] Getman I, Lopatin S. Theoretical and experimental investigation of the porous PZT ceramics. *Ferroelectrics*. 1996;186(1): 301-304.
[5] Iyer S, Venkatesh TA. Electromechanical response of (3–0, 3–1) particulate, fibrous, and porous piezoelectric composites with anisotropic constituents: A model based on the homogenization method. *Int. J. Solids Struct*. 2014;51(6): 1221-1234.
[6] Kara H, Ramesh R, Stevens R, Bowen CR. Porous PZT ceramics for receiving transducers. *IEEE Trans. Ultrason. Ferroelectr. Freq. Control*. 2003;50(3): 289-296.
[7] Kar-Gupta R, Venkatesh TA. Electromechanical response of porous piezoelectric materials. *Acta Materialia*. 2006;54(15): 4063-4078.
[8] Lee JK. An analytical study on prediction of effective properties in porous and non-porous piezoelectric composites. *J. Mech. Sci. Techn.* 2005;19(11): 2025-2031.
[9] Levassort F, Lethiecq M, Sesmare R, Tran-Huu-Hue LP. Effective electroelastic moduli of 3-3(0-3) piezocomposites. *IEEE Trans. Ultrason. Ferroelectr. Freq. Control*. 1999;46(4): 1028-1034.
[10] Martinez-Ayuso G, Friswell MI, Adhikari S, Khodaparast HH, Berger H. Homogenization of porous piezoelectric materials. *Int. J. Solids Struct*. 2017;113–114: 218-229.
[11] Mori T, Tanaka K. Average stress in matrix and average elastic energy of materials with misfitting inclusions. *Acta Metall*. 1973;21(5): 571-574.
[12] Nguyen BV, Challagulla KS, Venkatesh TA, Hadjiloizi DA, Georgiades AV. Effects of porosity distribution and porosity volume fraction on the electromechanical properties of 3-3 piezoelectric foams. *Smart Mater. Struct.* 2016;25(12): 125028.
[13] Ramesh R, Kara H, Bowen CR. Finite element modelling of dense and porous piezoceramic disc hydrophones. *Ultrasonics*. 2005;43(3): 173-181.
[14] Rittenmyer K, Shrout T, Schulze WA, Newnham RE Piezoelectric 3–3 composites. *Ferroelectrics*. 1982;4(1): 189-195.
[15] Rybyanets AN. Porous piezoceramics: theory, technology, and properties. *IEEE Trans. Ultrason. Ferroelectr. Freq. Control*. 2011;58(7): 1492-1507.
[16] Rybyanets AN, Rybyanets AA. Ceramic piezocomposites: modeling, technology, and characterization. *IEEE Trans. Ultrason. Ferroelectr. Freq. Control*. 2011;58(9): 1757-1773.
[17] Silva ECN, Fonseca JSO, Kikuchi N. Optimal design of periodic piezocomposites. *Comput. Meth. Appl. Mech. Eng*. 1998;159(1-2): 49-77.
[18] Topolov VY, Bowen CR. *Electromechanical Properties in Composites Based on Ferroelectrics.* London: Springer; 2009.
[19] Wersing W, Lubitz K, Mohaupt J. Dielectric, elastic and piezoelectric properties of porous PZT ceramics. *Ferroelectrics.* 1986;68(1): 77-97.
[20] Nasedkin AV, Shevtsova MS. Multiscale computer simulation of piezoelectric devices with elements from porous piezoceramics. In: Parinov IA, Chang SH. (eds.) *Physics and Mechanics of New Materials and Their Applications*. New York: Nova Science Publishers; 2013: p.185-202.
[21] Bobrov SV, Nasedkin AV, Rybjanets AN. Finite element modeling of effective moduli of porous and polycrystalline composite piezoceramics. In: Topping BHV, Montero G, Montenegro R. (eds.) *Proc. VIII Int. Conf. on Computational Structures Technology*, Stirlingshire, UK: Civil-Comp Press; 2006. Paper 107.

[22] Berlincourt DA, Cerran DR, Jaffe H. Piezoelectric and piezomagnetical materials and their function in transducers. In: Mason WP. (ed.) *Physical Acoustics: Principles and Methods*. 1st ed. New York: Academic Press; 1964. p.169-270.
[23] Dieulesaint E, Royer D. *Elastic Waves in Solids: Applications to Signal Processing.* Chichester, UK: Wiley & Sons Inc.; 1980.
[24] Chermergor TD. *Theory of Elasticity of Microheterogeneous Media*. Moscow: Nauka; 1977. (In Russian)
[25] Kudimova AB, Mikhayluts IV, Nadolin DK, Nasedkin AV, Nasedkina AA, Oganesyan PA, Soloviev AN. Computer design of porous and ceramic piezocomposites in the finite element package ACELAN. *Procedia Structural Integrity*. 2017;6: 301-308.
[26] Kurbatova NV, Nadolin DK, Nasedkin AV, Oganesyan PA, Soloviev AN. Finite element approach for composite magneto-piezoelectric materials modeling in ACELAN-COMPOS package. In: Altenbach H, Carrera E, Kulikov G. (eds.) *Analysis and Modelling of Advanced Structures and Smart Systems*. Ser. *Advanced Structured Materials*. Advanced Structured Materials book series (STRUCTMAT, volume 81). Singapore: Springer; 2018. p.69-88.
[27] Kudimova AB, Nadolin DK, Nasedkin AV, Oganesyan PA, Soloviev AN. Finite element homogenization models of bulk mixed piezocomposites with granular elastic inclusions in ACELAN package. *Mater. Phys. Mech*. 2018;37(1): 25-33.
[28] Dantziger AJ, Razumovskaya ON, Reznitchenko LA, Sakhnenko VP, Klevtsov AN, Dudkina SI, Shilkina LA, Dergunova NV, Rybyanez AN. *Multicomponent Systems of Ferroelectric Solid Solutions: Physics, Crystallochemistry, Technology. Design Aspects of Piezoelectric Materials*. Rostov-on-Don: Rostov State University Press; 2001. (In Russian)
[29] Wachtman Jr. JB, Tefft WE, Lam Jr. DG, Stinchfield RP. Elastic constants of synthetic single crystal corundum at room temperature. *J. Res. Natl. Bur. Std.-A, Physics and Chemistry*. 1960;64A(3): 213-228.
[30] Rybyanets AN, Konstantinov GM, Naumenko AA, Shvetsova NA, Makar'ev DI, Lugovaya MA. Elastic, dielectric, and piezoelectric properties of ceramic lead zirconate titanate/α-Al_2O_3 composites. *Phys. Solid State*. 2015;57(3): 527-530.
[31] Rybyanets AN, Naumenko AA, Konstantinov GM, Shvetsova NA, Lugovaya MA. Elastic loss and dispersion in ceramic-matrix piezocomposites. *Phys. Solid State*. 2015;57(3): 558-562.
[32] Iovane G, Nasedkin AV. Modal analysis of piezoelectric bodies with voids. I. Mathematical approaches. *Appl. Math. Model*. 2010;34(1): 60-71.
[33] Iovane G, Nasedkin AV. Modal analysis of piezoelectric bodies with voids. II. Finite element simulation. *Appl. Math. Model*. 2010;34(1): 47-59.
[34] Iovane G, Nasedkin AV. Coupled finite element acoustopiezoelectric analysis of piezomaterials with voids and ultrasonic transducers from porous piezoceramics. *J. Coupled Syst. Multiscale Dyn*. 2013;1(3): 393-403.
[35] Iovane G, Nasedkin AV. New model for piezoelectric medium with voids for application to analysis of ultrasonic piezoelectric transducers and porous piezocomposites. In: Parinov IA (ed.) *Advanced Nano- and Piezoelectric Materials and their Applications.* New York: Nova Science Publishers; 2014: p.145-170.